Supporting Information

A multi-site recognition molecularly imprinted solid-phase microextraction fiber for selective enrichment of three cross-class environmental endocrine disruptors

Yunli Duan, Zhigang Xu*, Zhimin Liu*

Faculty of Science, Kunming University of Science and Technology, Kunming 650500, China

***Corresponding Author:**

xuzgkmust@gmail.com (Z.G. Xu); lab_chem@126.com (Z.M. Liu)

1. The properties of the target analyte

Table S1 Physical-chemical properties and molecular structures of the target compounds

Analyte	CAS no.	Molecular weight	pKa (25 °C)	logKow	Molecular Structure
Bisphenol F (BPF)	620-92-8	200.23	pKa_1:7.55 pKa_2:10.80	2.91	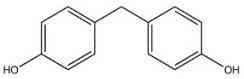
Diethyl phthalate (DEP)	84-66-2	222.24	7.84	2.47	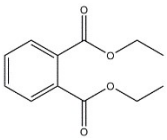
Methyl paraben (MP)	99-76-3	152.15	8.17	1.96	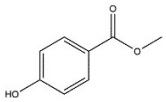

2. Characterization

Table S2. The AFM characterization parameters of MIP and NIP fibers

Fibers	Rq	Ra	Rz	Surface area
MIP	6.9 nm	4.8 nm	92.1 nm	4.0 μm^2
NIP	2.6 nm	1.6 nm	65.4 nm	4.0 μm^2

The Fourier transform infrared (FT-IR) of MIP and NIP fibers are shown in Figure S1. In the two similar spectral curves, the flexing vibration absorption peak of the hydroxyl group at the wavelength of 3456 cm^{-1} may be generated by the adsorbed water. The C–H characteristic absorption peak of alkanes corresponded to the wavelength of 2956 cm^{-1}. The carbonyl stretching vibration caused the characteristic absorption peak at 1730 cm^{-1}, while the peak at 1155 cm^{-1} was attributed to the characteristic absorption peak of C–O. The results revealed that there was no remarkable discrepancy between the FT-IR spectra of MIP and NIP fibers, indicating that the functional group composition of the two was similar. These findings indirectly explained the interaction between the template molecule and the functional monomer on the polymer during the synthesis of the MIP fiber. The action relied on weak hydrogen bonding forces.

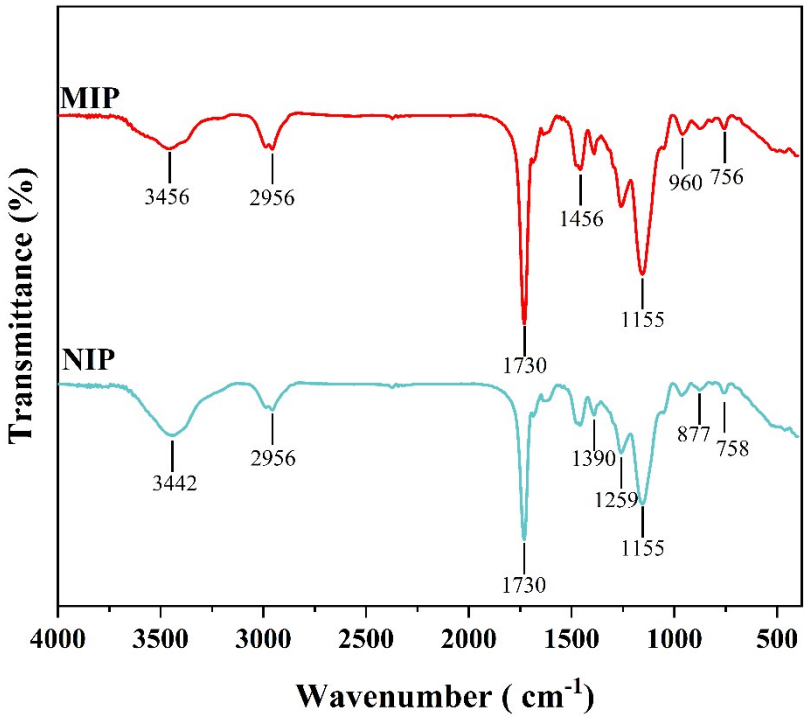

Fig. S1 FT-IR spectra of MIP and NIP fibers.

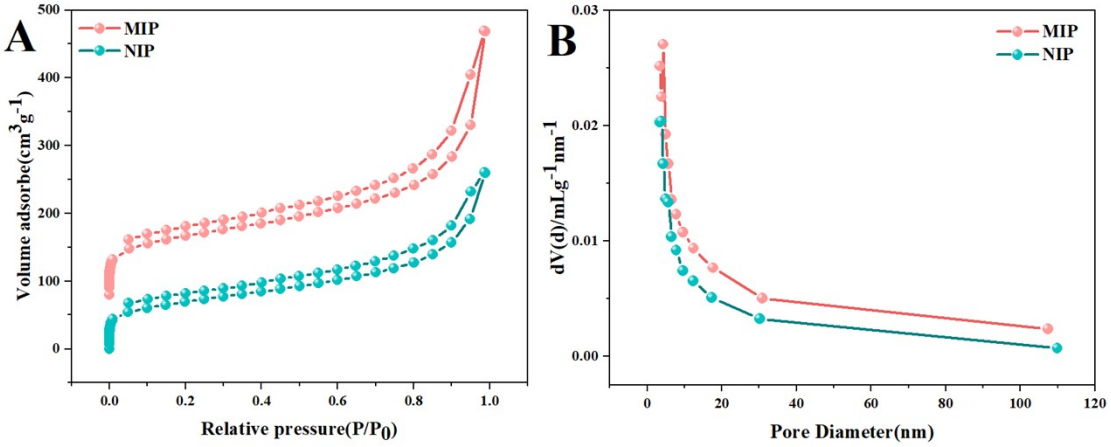

Fig. S2 (**A**) N_2 adsorption–desorption isotherms, (**B**) pore size distribution of MIP and NIP.

Table S3 Brunauer-Emmett-Teller (BET) measurement surface area and pore parameters

Fibers	Surface area (m^2/g)	Average pore Diameter (nm)	Total pore volume (cm^3 /g)
MIP	307.21	7.83	0.60
NIP	295.52	6.59	0.40

3. Study on the adsorption isotherm model

The Scatchard model was used to describe the binding properties of multi-site recognition MIP and NIP fibers to BPF, DEP and MP. As shown in Table S4, the K_d and Q_{max} values of the fibers are determined by the slope and intercept of the two linear parts of the Scatchard plot, respectively, which are important parameters for studying the adsorption properties of MIP and NIP during the binding process and for distinguishing the recognition sites.

Table S4 Scatchard analysis of MIP and NIP fibers

Fibers	Analytes	Low-affinity sites		High-affinity sites	
		K_d (mmol/L)	Q_{max} (mmol/g)	K_d (mmol/L)	Q_{max} (mmol/g)
MIP	BPF	7.77×10^{-4}	2.26×10^{-2}	1.13×10^{-4}	6.1×10^{-3}
	DEP	1.10×10^{-3}	2.06×10^{-2}	6.90×10^{-5}	3.06×10^{-3}
	MP	3.61×10^{-3}	2.09×10^{-2}	5.31×10^{-4}	4.97×10^{-3}
NIP	BPF	2.14×10^{-3}	1.70×10^{-2}	/	/
	DEP	7.83×10^{-4}	3.04×10^{-3}	/	/
	MP	2.12×10^{-2}	5.21×10^{-2}	/	/

The Langmuir and Freundlich adsorption isotherm equations are as follows:

$$Q_e = \frac{Q_M K_L C_e}{1 + K_L C_e} \quad (1)$$

$$Q_e = K_F C_e^{1/n} \quad (2)$$

Where C_e is the concentration of the equilibrium solution, μg/L; Q_e is the equilibrium adsorption capacity, μg/g; Q_M is the theoretical maximum adsorption capacity, μg/g; K_L is the equilibrium constant of the Langmuir model. With Q_e as the ordinate and C_e as the abscissa, Langmuir nonlinear fitting was

performed. The fitting results can obtain the K_L and the Q_M.

In equation (2), K_F is the adsorption coefficient of Freund equilibrium, indicating the relationship between adsorption capacity and adsorption energy. The values of K_F and n are only related to the adsorbent, the type and temperature of the adsorbate, and they are empirical constants. The value of n indicates the difficulty of adsorption. All of parameters can be obtained by fitting different isotherm model as above to experimental adsorption data.

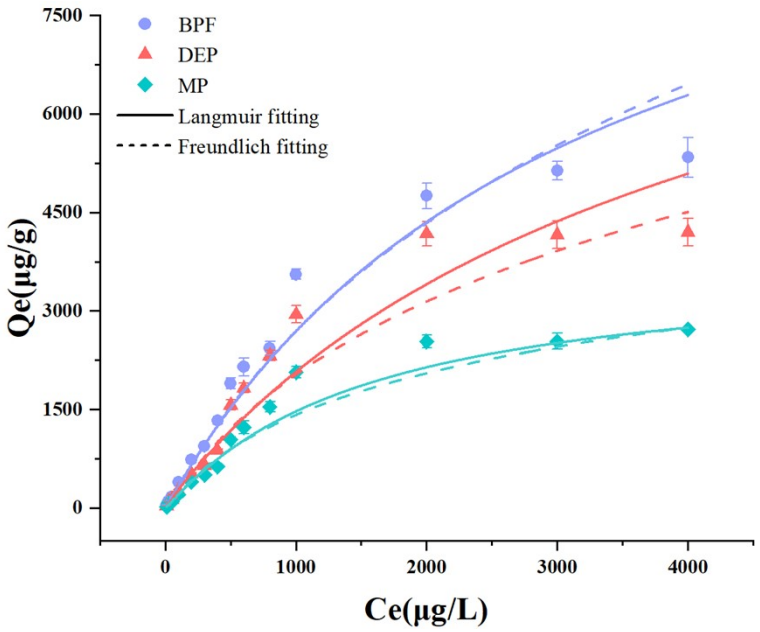

Fig. S3 Langmuir and Freundlich fitting curves for MIP fiber to BPF, DEP and MP.

Table S5 Parameter analysis of two adsorption models

Analytes	Langmuir model			Freundlich model		
	Q_M (μg/g)	$K_L \times 10^{-4}$	R^2	K_F	n	R^2
BPF	11192.51	2.97	0.9919	8.20	1.21	0.9912
DEP	10640.06	3.15	0.9774	4.96	1.15	0.9698
MP	3720.98	4.58	0.9889	5.11	1.31	0.9864

4. Selectivity study

The extraction rate, desorption rate, imprinting factor (IF) and enrichment factor (EF) were calculated by the following equations (3)-(6).

$$\text{Desorption } rate(\%) = \frac{m_1}{m_2} \times 100\% \quad (3)$$

$$\text{Extraction } rate(\%) = \frac{m_2}{m_0} \times 100\% \quad (4)$$

$$IF = Q_{MIP}/Q_{NIP} \quad (5)$$

$$EF = \frac{C_f}{C_i} \quad (6)$$

where m_1 is the mass of the analyte desorbed from each fiber for the first time; m_2 is the total mass of the analyte desorbed from each fiber. m_o is the total mass of the analyte in the solution before extraction. Q_{MIP} and Q_{NIP} represent the adsorption capacity of MIP and NIP, respectively. C_i (μg/L) is the initial concentration before extraction and C_f (μg/ L) is the concentration of analytes in the desorption solvent. All of these parameters for assessing specific recognition properties are summarized in Table S6.

Table S6 Parameters of specific recognition properties of MIP and NIP fibers

Analytes		Extraction rate (%)		Desorption rate (%)		IF	EF
		MIP	NIP	MIP	NIP		
Target analytes	BPF	89.73	58.12	84.09	82.88	1.55	224.33
	DEP	61.48	36.47	81.26	84.33	1.69	153.69
	MP	47.42	27.35	80.57	86.84	1.75	118.56
Structural analogs	BPA	68.91	41.74	85.75	83.97	1.65	198.79
	DMP	31.14	27.41	89.91	91.84	1.14	115.13
	EP	38.97	21.52	88.76	85.66	1.81	104.83
Non-structural analogs	An	1.50	1.59	57.01	72.58	0.94	3.74

	BnOH	7.97	7.98	73.48	81.51	1.00	19.94
	2-NP	11.64	11.63	67.52	75.18	1.00	29.10

Table S7 Molecular size of target analytes, structural analogs, and non-structural analogs

Analytes		Molecular three-dimensional size (Å)	Arithmetic mean radius (Å)	Geometric mean radius (Å)	Geometric configuration
Target analytes	BPF	12.072×7.178×5.480	4.122	3.901	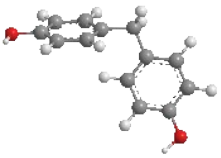
	DEP	11.177×8.378×6.039	4.266	4.135	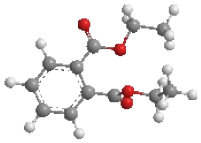
	MP	10.743×6.697×4.018	3.576	3.306	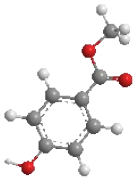
Structural analogs	BPA	12.274×7.556×6.501	4.388	4.224	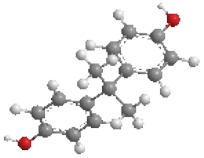
	DMP	9.822×8.051×5.274	3.858	3.736	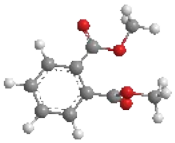
	EP	12.289×6.931×4.019	3.873	3.498	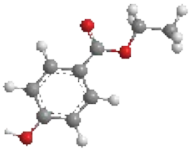
Non-structural analogs	An	7.881×6.522×3.201	2.934	2.740	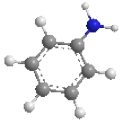
	BnOH	9.102×6.998×4.019	3.353	3.175	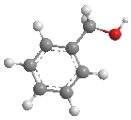
	2-NP	8.366×7.481×3.201	3.175	2.926	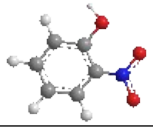

5. Environmental water sample analysis

Table S8 Linear range, linear equation, and correlation coefficient of the MIP fiber combined with HPLC-DAD method for the detection and analysis of BPF, DEP, and MP

Analytes	Linear range (μg/L)	Linear equation	R	LOD(μg/L)	LOQ(μg/L)
BPF	0.01-200.00	y=0.1834x+0.4996	0.9992	0.003	0.01
DEP	0.05-200.00	y=0.1324x+0.3680	0.9994	0.020	0.05
MP	0.01-200.00	y=0.1382x+0.4071	0.9992	0.003	0.01

Table S9 Analysis of BPF, DEP, and MP in three environmental water samples (n = 3)

Samples	Analytes	Found μg/L	Spiked Analysis					
			1.00 μg/L		25.00 μg/L		100.00 μg/L	
			Recovery (%)	RSD (%)	Recovery (%)	RSD (%)	Recovery (%)	RSD (%)
Sample 1	BPF	0.72	89.98	7.89	109.40	4.33	108.08	6.27
	DEP	/	106.77	2.30	107.34	2.66	103.12	5.24
	MP	0.38	75.76	4.74	94.46	8.43	96.51	3.48
Sample 2	BPF	/	89.44	3.02	109.11	7.25	112.69	5.20
	DEP	/	93.99	8.27	100.90	10.40	109.26	6.45
	MP	/	102.22	3.23	100.68	4.54	97.85	3.68
Sample 3	BPF	/	80.58	5.41	95.68	6.78	110.60	4.27
	DEP	/	109.00	2.97	100.56	11.46	92.55	4.36
	MP	/	101.81	3.31	86.05	3.24	101.73	10.83

"/" means not found.

Table S10 Comparison of the present method with previously reported methods

Methods		Analytes	Matrix	Detection method	Liner range (μg /L)	Limit of detection (μg/L)	Speed (rpm)	Enrichment factor	Ref.
Conventional methods	GONRs-HF-SLPME	Five bisphenol compounds	Plastic bottled drinking water, carbonated beverage and canned beer	HPLC-PDA	1–1500	0.1–0.4	900	76–127	1
	TF-SPME	Five endocrine disruptors	River water	HPLC-DAD	5–285	1–8	–	–	2
	SDME	Six endocrine disruptors	Environmental water samples	HPLC-PDA	1–1000	0.33–0.67	700	147–289	3
	SLSC-ME	Five bisphenol compounds	Environmental water samples	HPLC-UV	1–500	0.20–0.90	–	74–128	4
	MDSPME	Eleven endocrine disruptors	Sea, river, and swimming-pool water	HPLC-MS/MS	0.5–500	0.16–1.35	750	15.4–49.2	5
	DLLME	Bisphenol A	Municipal wastewater	GC-MS	1.0–500	0.33	–	–	6
MIP methods	Mag-MIPs	Two estrogens	Environmental water samples	FAPA-MS	0.027–27	0.135	–	–	7
	SMIP-SBSE	Three endocrine disruptors	Environmental water samples	HPLC-DAD	0.1–200	0.004–0.01	–	25–122	8
	MIP-SPME	Three endocrine disruptors	Environmental water samples	HPLC-DAD	0.01–200.00	0.003–0.02	500	118.6–224.3	This work

GONRs-HF-SLPME: graphene oxide nanoribbon-reinforced hollow fiber solid/liquid phase microextraction; TF-SPME: thin-film solid-phase microextraction; SDME: single drop microextraction; SLSC-ME: solid-liquid-solid conversion microextraction; MDSPME: magnetic dispersive solid phase microextraction; Mag-MIPs: Magnetic molecularly imprinted polymers; DLLME: Dispersive liquid-liquid microextraction; SMIP-SBSE: supramolecular imprinted polymeric stir bar sorptive extraction; MIP-SPME: molecularly imprinted polymer solid phase microextraction.

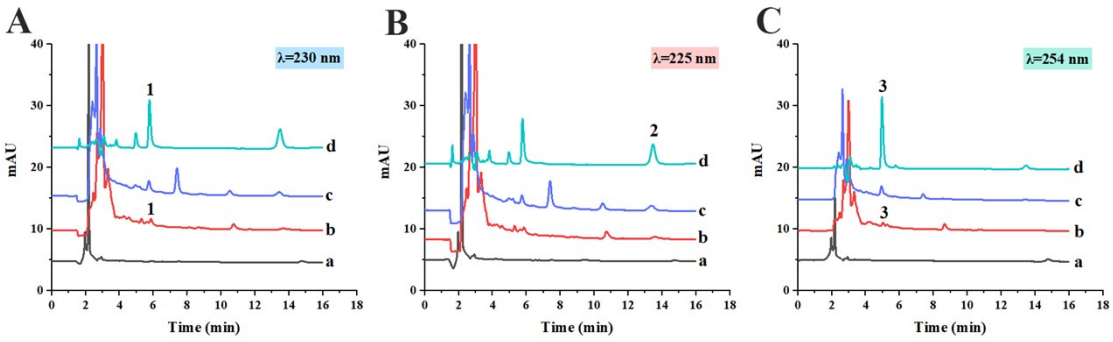

Fig. S4 Chromatograms of sample 1. (A) Chromatogram at 230 nm; (B) chromatogram at 225 nm; (C) chromatogram at 254 nm; (a) sample 1 direct injection; (b) extracted sample 1 by MIP; (c) MIP extracted spiked 1 μg/L sample 1; and (d) 1 mg/L mixed standard solution: 1. BPF, 2. DEP, and 3. MP.

References

1. X. Han, J. Chen, H. Qiu and Y.-P. Shi, *Microchim. Acta*, 2019, **186**, 375.
2. N. Kirschner, A. N. Dias, D. Budziak, C. B. da Silveira, J. Merib and E. Carasek, *Anal. Chim. Acta*, 2017, **996**, 29-37.
3. Y. H. Jiang, X. L. Zhang, T. T. Tang, T. S. Zhou and G. Y. Shi, *Anal. Lett.*, 2015, **48**, 710-725.
4. X. Chen, L. Wei, Q. Liu and J. Zhao, *Microchem. J.*, 2021, **169**, 106538.
5. F. A. Casado-Carmona, M. d. C. Alcudia-León, R. Lucena, S. Cárdenas and M. Valcárcel, *Microchem. J.*, 2016, **128**, 347-353.
6. D. S. Chormey, Ç. Büyükpınar, F. Turak, O. T. Komesli and S. Bakırdere, *Environ. Monit. Assess.*, 2017, **189**, 277.
7. M. Guc and G. Schroeder, *Biomolecules*, 2020, **10**, 672.
8. Z. Liu, Z. Xu, Y. Liu, Y. Liu, B. Lu and L. Ma, *Microchem. J.*, 2020, **158**, 105163.